

MULTI-MEASUREMENT CORRELATIONS IN THE NEAR-FIELD OF A COMPLEX SUPERSONIC JET USING TIME-RESOLVED SCHLIEREN IMAGING

Andrew S. Tenney

Department of Mechanical and Aerospace Engineering
Syracuse University
263 Link Hall, Syracuse NY 13244
astenney@syr.edu

Thomas J. Coleman

Department of Mechanical and Aerospace Engineering
Syracuse University
263 Link Hall, Syracuse NY 13244
thcolema@syr.edu

Jacques Lewalle

Department of Mechanical and Aerospace Engineering
Syracuse University
263 Link Hall, Syracuse NY 13244
jlewalles@syr.edu

Sivaram Gogineni

Spectral Energies, LLC
Dayton OH, 45431
goginesp@gmail.com

Abstract

In this study, we aim to characterize the dynamics and visualize the propagation of fluctuations in the near field of a complex multi-stream jet over an aft deck plate. The flow is visualized using time resolved schlieren photography (up to 400,000 frames per second) while pressure on the aft deck plate is simultaneously sampled using Kulite pressure sensors. Time series are constructed using the schlieren photographs and conditioned to reduce the effects of signal drift. The analysis is focused in several regions identified in previous studies as dynamically interesting through their high levels of pressure variance and rich spectral content. Space-Time cross correlations are utilized to visualize propagation of fluctuations from the near field to the far field, and several propagation pathways are identified. This process is repeated for band-pass filtered schlieren signals, and a case is made for the separability of near field dynamics into distinct frequency bands.

Introduction

Over the last several decades, performance requirements of both commercial and military aircraft have led to increasingly complex propulsion systems, often including rectangular multi-stream nozzle configurations. Only within the last few years has noise become a design parameter for propulsion and airframe engineers [1]. While a complete theoretical understanding of jet noise has remained elusive, there is a wealth of information on which to build our knowledge base. There is a large number of theoretical and experimental studies focused on the flow regimes

with which this study deals.

In his 1991 chapter in *Aeroacoustics of Flight Vehicles* [2], Tam gives a thorough description of possible acoustic sources in the near field of supersonic jets. He highlights the importance of large scale motions in noise production where M_j (jet Mach number) is greater than 1. Of particular interest are the phenomena of Mach wave radiation and broadband shock associated noise, particularly because they have firm theoretical descriptions [3], [4], and will be prominent sources of noise in our experiment due to our chosen design conditions. In addition to the fundamental theoretical and experimental work outlined in [2], more recent applied work has been performed by Bridges cataloging the acoustic character of pure rectangular jets [5] and those exhausting over flat plates. In the aforementioned study, it was shown that noise increases with deck length and that the deck edge acts like a dipole in its velocity scaling and directivity [6].

The goal of the present study is to utilize time resolved schlieren photography to observe and characterize the near-field phenomena contributing to far-field noise, as described in the existing literature. With this time resolved view of the near-field, we hope to make more reliable predictions about far-field noise, particularly in the complex flows seen in modern day and next-generation aircraft exhaust.

To this end, a multi-stream supersonic jet flow is visualized with a time-resolved schlieren system. In the lab, this complex flow is simplified, and is represented by a main flow, a wall jet along the aft deck plate, and a low-speed co-flow to mimic modest forward motion. The aft deck plate is configurable to several different lengths. The general con-

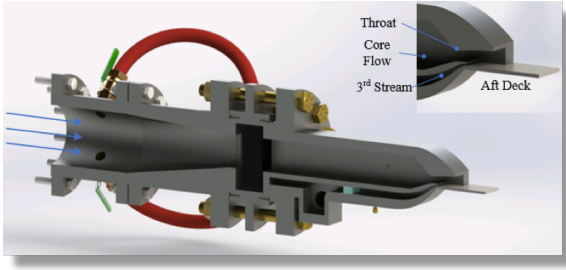


Figure 1. Rendering of MARS nozzle at Syracuse University. [7]

figuration is captured in Fig. 1. The Mach number of the main flow can be varied from 1.0 to 1.6, while the wall jet can be varied from Mach 0.6 to 1.0. These settings encompass the main interaction flow regimes. In the current study, nozzle pressure ratios corresponding to a Mach 1.6 main flow and Mach 1.0 wall jet are examined.

Instrumentation

All experiments in this study were conducted within Syracuse University's anechoic chamber. A time-resolved schlieren system was developed to capture the transient structures within this complex nozzle flow. Time resolution was deemed necessary to analyze the relatively short timescale and high-frequency phenomena that occur in the near field, as well as to perform high-quality cross-correlations within the flow-field. To achieve reasonable time resolution, a Photron FASTCAM SA-Z was used in conjunction with a 2100 lumen overdriven Luminus CBT-120 green LED [8], [9] and two high-quality sister parabolic mirrors. With our chosen setup, we are able to achieve frame-rates from 50,000 to 400,000 frames per second, with window sizes up to 12.5 inches in diameter (please see [10] for full experimental detail, including facility description and schematics).

In addition to these optical methods, an array of Kulite pressure sensors was embedded in the aft deck of the jet nozzle, and were sampled at 100kHz.

1 Methodology and Analysis

1.1 Time-Frequency and Spectral Tools

In our analysis, we utilize both spectral and time-frequency tools, or more specifically, the Fourier spectrum and the Morlet wavelet transform and its associated spectrum. The Morlet wavelet was chosen due to the good spectral resolution it provides. By using both of these methods, we are able to examine the frequency content of the signals we construct from the schlieren images. The wavelet itself consists of a Fourier wave of unit frequency, modulated by a Gaussian envelope of which the relative width is controlled by the parameter z_0 .

$$\Psi_{M,z_0}(t) = e^{-2\pi^2 t^2 / z_0} (e^{2i\pi t} - e^{-\frac{2}{z_0}}). \quad (1)$$

Changing the wavelet's frequency is done by using a dimensional time t and a chosen frequency ω , together with

appropriate scaling:

$$\Psi_M(t\omega) = \frac{\omega}{\sqrt{c_\Psi}} \Psi_{M,z_0}(t\omega). \quad (2)$$

The transform is performed via a convolution with the original time series, and is given by the integral:

$$\tilde{p}_M(t, \omega) = \int p(t') \Psi_M^*((t-t')\omega) dt'. \quad (3)$$

The corresponding spectrum is then given by:

$$E_M(\omega) = \frac{1}{2} \int |\tilde{p}_M|^2. \quad (4)$$

As the value of z_0 is increased towards infinity, the Gaussian envelope expands, and the wavelet transform approaches the Fourier transform. At the commonly used value of $z_0 = 0.5$, however, the wavelet spectrum tends to distribute energy over wider bands, and therefore, some of the narrow peaks present in the Fourier spectra get smoothed out. This provides a good overall illustration of the trends in the spectrum at the expense of some detail. In contrast, the Fourier spectrum shows significant scatter. In signals with high amounts of local periodicity in addition to a broad band spectrum, peaks of interest are sometimes difficult to pick out. To better identify frequencies that could be playing a role in the flow physics, we take the ratio of the Fourier spectrum to the Morlet spectrum, and look for frequencies for which this ratio is substantially higher than 1. As a variation of this process (that removes the need to interpolate the Morlet spectrum onto the more highly resolved vector of frequencies in the DFT), we can compare a well-resolved Morlet spectrum with a low value of z_0 to one with a much higher value, such that it approximates the Fourier spectrum. An example of this can be seen in Fig. 2.

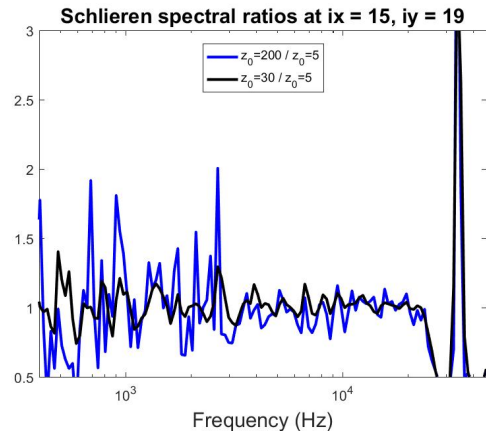


Figure 2. Ratio of Morlet spectrum with $z_0 = 200$ to $z_0 = 5$ (blue) and $z_0 = 30$ to $z_0 = 5$ (black)

1.2 Time Series from Schlieren Images

The time resolution of the schlieren images allows us to build time series by tracking the temporal evolution of gray

shades at individual points in the flow field (as described in [10]). A schematic of the process can be seen in Fig. 3. It is important to recall that span-wise structures will be enhanced in cross stream views because schlieren imaging integrates difference in refractive index across the flow. Qualitatively, sporadic coherence and entrainment can be observed using only the naked eye, particularly in the upper and lower free shear layers, and should therefore be detectable quantitatively using careful analysis.

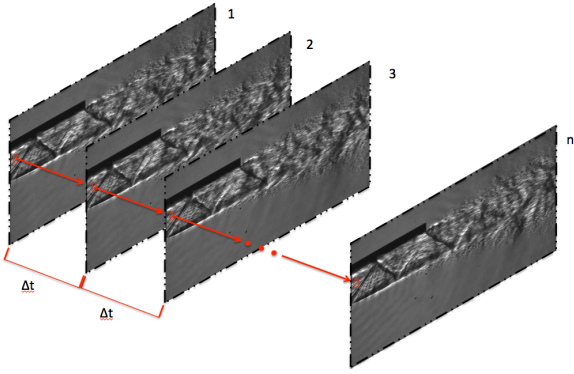


Figure 3. Schematic of creating time series from schlieren images

Using the methods described in [10], we have collected simultaneous time traces of grey-shade fluctuations at various locations in the flow. In previous work, we have performed preliminary processing with the algorithms used for the treatment of time-resolved PIV data and of LES data [11], [12]. Unfortunately, due to tiny differences in LED-camera synchronization and limited dynamic range of the photographic sensor, portions of time traces exhibit some clipping and we see average pixel intensity drift over the entirety of the field. We argue that in most regions, the affect of clipping on the signal’s spectrum is minimal, and can therefore be ignored, while intensity drift is processed out.

To combat this drift, we employ a non-linear detrending method, assisted by the dominance of the 34kHz oscillations [10] in the signals. The signals are band-pass filtered around 34kHz using the Morlet wavelet transform, and the location of consecutive peaks are noted. Zero crossings are estimated at the one-quarter and three-quarter local period points, as determined by the separation of these consecutive peaks. The values of the original signal at the times of these zero crossings are then recorded, and connected via a linear interpolation between them. This curve is then smoothed via a Gaussian filter, resulting in an approximate low frequency trendline of the data. This trend can be subtracted from the data to produce a reasonable approximation of the time-trace without the varying light intensity. An example of the effects of this detrending on the signal spectrum is shown in Fig. 4. Note that the increase in spectral amplitude is attributed to a renormalization of the signal to zero-mean, unit-variance after the trend line has been subtracted. Low frequency detrending primarily affects frequencies below 100Hz, with reasonably minimal effects on the middle band, and slight roll off of the highest frequencies. The overall shape and location of spectral peaks remain unaltered.

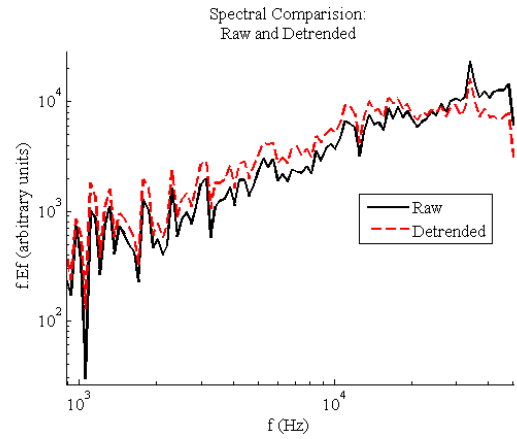


Figure 4. Comparison of raw and detrended signal compensated spectra.

In addition to this direct comparison, we must also confirm that the cross correlations are not negatively affected by this detrending. Four examples are shown side by side in Fig. 5: raw signals in the left column and detrended signals in the right, with identical color scales. As you can see, the correlation maps are nearly identical in both cases. In some instances, detrending sharpens the regions of high correlation and makes their propagation paths clear. From these comparisons, we argue that the cross correlations are at least qualitatively not strongly affected by the detrending. In the cases where there is a difference, the detrending has a positive effect on correlation values.

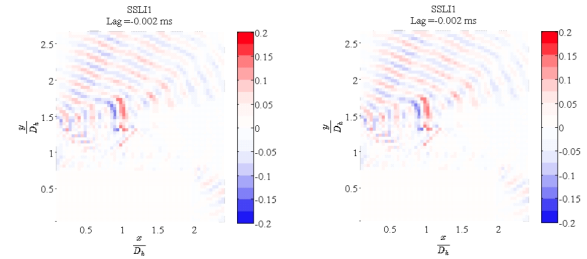


Figure 5. Comparison of raw and detrended full-field correlations. Left: saw signals; Right: detrended signals

1.3 Space-Time Cross Correlations

To assist in the visualization of the propagation of information in the flow, we use a technique that we call space-time correlation. This technique was developed by P. Kan and is described in detail in [13]. In this technique, a reference signal from a point of interest is cross correlated with all other points in the flow field. In our analysis, these points (referenced in Fig. 6) were defined by looking for the pixels in the schlieren field with the highest RMS noise. These points roughly corresponded to the near-field “hotspots” defined by Kan et al. [13]. In an analysis of single-plane LES data, it was shown that this method proved as a useful tool in visualizing and tracking regions of high correlation as they propagate through the flow field. Because of the integrated

nature of schlieren images, it is expected that these correlations would be substantially weaker. We hypothesize that if the density variations are strong enough and persist both spatially and temporally, then similar fluctuation propagation patterns should be observed.

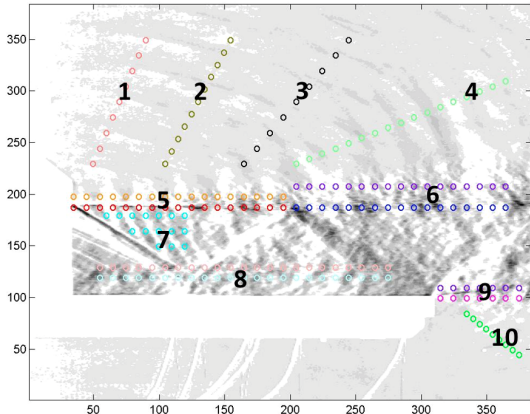


Figure 6. Regions of interest in schlieren snapshots

In the same vein as the above mentioned analysis, this process can also be performed on band-pass filtered signals from the near field. The frequencies at which we choose to band-pass filter are identified using the Fourier-Morlet ratio described in the previous section. In using this method, we choose not to re-normalize the band-pass filtered signals when we cross correlate them. By eliminating this step, we are calculating the contribution to the overall correlation coefficient by an individual frequency band. The full coefficient can be recovered by a summation of these frequency-specific coefficients.

2 Results

2.1 Statistics in the Schlieren Field

While schlieren images as a whole relate to density variation within a flow field, without the use of background orientation [14], the grey shades in the images cannot be tied to any physical value. For this reason, all time series are normalized to zero-mean and unit variance. Power spectra are calculated for each of the spatial points sampled. In all series of spectra with clear axial sequences, the sequence is blue to red (upstream to downstream).

To begin to differentiate and classify regions in the near field based on differing dominant physics, we choose to look at their Morlet spectra. By visual inspection, the region most physically distinct from the turbulent jet itself is the near-acoustic field just above and below the plume. In these regions, the dominant physical phenomenon is acoustic radiation, presumably driven by three different hydrodynamic phenomena: Mach wave radiation, fine scale turbulence, and shock-shear layer interactions (leading to broad-band shock associated noise, or BBSAN [4]). Morlet spectra of signals from this region are detailed in Fig. 7. Two major spectral features are apparent: a low-to-mid frequency broadband peak, and a sharp, distinct peak at $St = 3.4$ (where $St = fD_h/U_{jet}$). The broadband peak is presumably associated with BBSAN, as it is in the correct range for this phenomenon. This sharp peak appears in the spectra

of all other regions of the jet (with varying relative amplitude), not just those dominated by acoustic radiation, and has been attributed to a Kelvin-Helmholtz-like instability forming just aft of the splitter plate separating the wall jet from the main flow [15]). These general trends are common throughout the spectra in all regions, however the details differ depending on the dominant physics. This highlights the complexity of the flow and lends insight into the underlying physical mechanics in each distinct region.

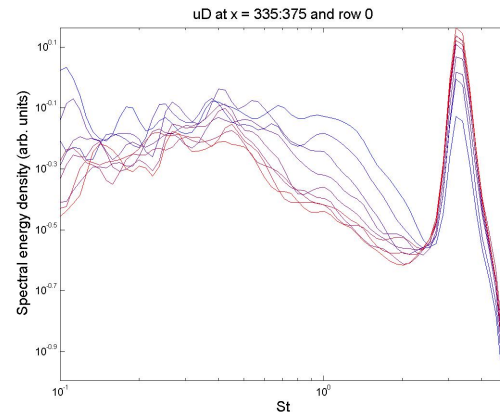


Figure 7. Uncompensated Morlet spectra of schlieren signals in the uD region. Blue - Red corresponding to Upstream - Downstream.

2.2 Full-Field Correlations

By correlating a point roughly corresponding to the interaction of the first compression shock with the upper free shear layer, we find reasonably high regions of correlation. These pockets of correlation originate near the lip of the jet and travel towards the reference point. After they pass this point, they split into 3 distinct packets of correlation and travel along 3 different propagation paths: along the reflected expansion wave, along the upper free shear layer, and towards the far field in the near-acoustic region. This progression is shown in Fig. 8, with lag increasing from left to right and top to bottom, respectively. Similar patterns have been shown by Kan et al. [13], and such a distinct pattern in the cross correlations of the schlieren field seems to support our hypothesis that strong enough regions of density variation would be objectively identifiable.

In the case shown in Fig. 9 (identical lag progression pattern as in Fig. 9), a signal just slightly downstream of the aft deck is used as the reference signal. With this reference, we see packets of correlation originating in the inner shear layer and just above the deck plate travelling downstream. As they reach the deck lip, they seem to produce acoustic waves that radiate downwards. This radiation is in accordance with that described by Powell [16] and Bridges [6].

2.3 Band-Pass Filtered Full-Field

By band-pass filtering the Schlieren Signals, we see how information is moved around within the flow at specific frequencies. As a guide, we use the frequencies defined by our spectral ratio plots (see Fig. 2). The first frequency around which we filter is 34kHz, corresponding to

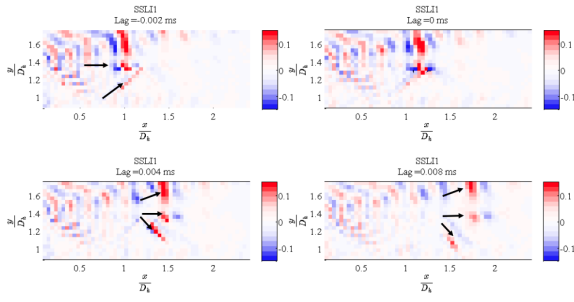


Figure 8. Space-time correlations. Full-field with Shock-Shear Layer Interaction 1 (SSLI1)

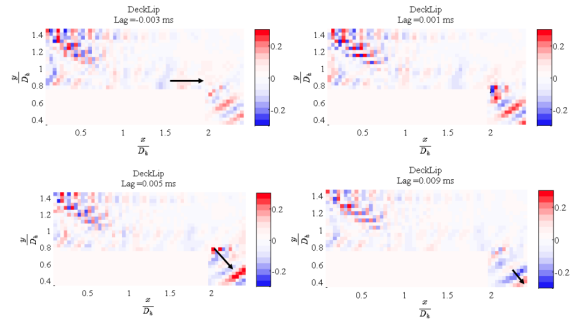


Figure 9. Space-time correlations. Full-field with lip of aft deck

the largest peak of the Fourier-Morlet spectral ratios in Fig. 2, and we once again look at the first shock-shear layer interaction (Fig. 10). At this frequency, we no longer see the propagation of individual correlation packets as they travel within the flow. We do however, see that regions the field correlate well over almost all time lags with this reference point. This trend was expected, due to the ubiquity and dominance of the 34kHz frequency throughout all the schlieren signals.

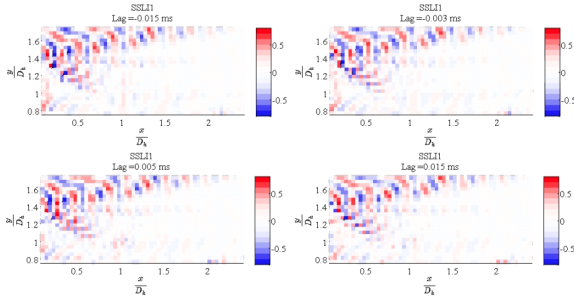


Figure 10. Band-pass filtered space-time correlations. Full-field with SSLI1 at 34kHz

This process can be repeated at other frequency bands, however, the results are more difficult to interpret. Since the 34kHz is so dominant in the signals, individual, less energetic, frequency bands tend to have less of an impact on overall correlation.

3 Conclusions and Future Studies

The use of time series generated from time-resolved schlieren photography has so far proved both fruitful and promising. We have shown that signal drift in these images can be mitigated to some degree by finding a non-linear trendline in the data and subtracting it. By applying the space-time correlation method outlined in [13], we have been able to identify and track regions correlating well to a reference signal as they propagate through the flow field. Over all, the most common paths of propagation appear to be in the free shear layer at the upper limit of the jet, in the quiescent fluid above this free shear layer, in the inner shear layer separating the primary and tertiary streams, and along the oblique shock and expansion waves in the core flow. These propagation paths are in accordance with those found in [13], and what we have expected from previous analysis. In addition, hydrodynamic events that propagate within the flow over the deck have been shown to be well correlated with acoustic emissions off the lip of the deck plate in accordance with [6], [16]. By band pass filtering the signals around frequencies of interest, we have illustrated the varying importance of different frequency bands and have begun to isolate the modes of propagation to specific frequencies. This analysis has provided us with a basic understanding of the way information is spread throughout the near field, and will provide a jumping off point for future, more detailed, studies.

From this and the study presented in [17], it seems that we may be able to apply event-finding methods to the schlieren signals and the accompanying kulite pressure traces. The gray-shade signals from schlieren data, and kulite signals from the vicinity of the shear layers, will be processed through our wavelet transform and pattern recognition algorithms. In the analysis of axisymmetric jet data sets, these algorithms have proven useful in identifying energetic acoustic events in several far-field microphones as well as tying near-field hydrodynamic events to their associated far-field signatures [11]. While these methods have not yet been applied to schlieren, the results presented here give us reason to believe that they may be useful, given the ability of our cross correlation scheme to identify the propagation of information in the flow. These tools coupled with our high sampling rate may give us unique insight into the spatio-temporal evolution of large noise producing structures in the flow and their ties to noise generation.

4 Acknowledgements

This work has been funded by AFOSR grant number FA9550-15-1-0435 (program manager Dr. Douglas Smith), Spectral Energies, LLC, and an SBIR grant from AFRL. Partial support was also provided by Syracuse University. Special thanks to TJ Coleman, Andrew Magstadt, and Matthew Berry for all the time spent in the lab getting these data sets, Han Pham for her contributions to its analysis, and my advisors, Dr. Mark Glauser and Dr. Jacques Lewalle.

REFERENCES

- [1] Powell, Clemans A., Preisser, John S., NASA's Subsonic Jet Transport Noise Reduction Research, *NASA Technical Report Server*, Published 2000, accessed January 2017
- [2] Tam, C.K.W., *Jet Noise Generated by Large-Scale Co-*

- herent Motion, *Aeroacoustics of Flight Vehicles: Theory and Practice*, Vol. 1: Noise Sources, Ch 6. pp. 311-390, 1991.
- [3] Tam, Christopher K. W., Directional Acoustic Radiation from a Supersonic Jet Generated by Shear Layer Instability, *J. Fluid Mech.* vol. 46, pt. 4, April 27, 1971, pp. 737-768
- [4] Tam, C.K.W. and Reddy, N.N., Prediction Method for Broadband Shock-associated Noise from Supersonic Rectangular Jets, *Journal of Aircraft*, Vol. 33/2, pp. 298-303, 1996.
- [5] Gutmark, E., Schadow, K. C. and Bicker, C. J., Near Acoustic Field and Shock Structure of Rectangular Supersonic Jets, *AIAA Journal*, Vol. 28, No. 7, pp. 1163-1170, 1990.
- [6] Bridges, J. E., Noise from Aft Deck Exhaust Nozzles - Differences in Experimental Embodiments, 52nd AIAA ASM, AIAA-2014-0876, National Harbor, MD, 13-17 Jan. 2014.
- [7] Magstadt, A.S. and Berry, M.G. and Shea, P.R. and Glauser, M.N. and Ruscher, C.J. and Gogineni, S.P. and Kiel, B.V., Aeroacoustic Experiments on Supersonic Multi-aperture Nozzles, 51st AIAA Joint Propulsion Conference, Orlando, FL, 27-29 July 2015
- [8] Wilson, S., Gustafson, G., Lincoln, D., Murari, K., and Johansen, C., Performance evaluation of an overdriven LED for high-speed Schlieren imaging, *The Visualization Society of Japan* (2015) 18:35-45
- [9] Willert, C., Mitchell, D., Soria, J., An assessment of high-power light-emitting diodes for high frame rate Schlieren imaging, *Exp Fluids* (2012) 53:413-421
- [10] Tenney, A.S., Coleman, T.J., Lewalle, J., Glauser, M.N., Kiel, B.V. and Gogineni, S.P., Identifying Coherent Structures in a 3-Stream Supersonic Jet Flow Using Time-Resolved Schlieren Imaging, SciTech paper ref. no 2322032, 2016.
- [11] Kan, Pingqing, Lewalle, Jacques and Daviller, Guillaume, Comparison of Near Field Events and Their Far-Field Acoustic Signatures in Experimental and Numerical High Speed Jets, *Eighth International Symposium on Turbulence and Shear Flow Phenomena*, Poitiers, Futuroscope, France, August 28-30, 2013
- [12] Kan, P., Lewalle, J., Glauser, M.N., Gogineni, S.P. and Kiel B.V., Extracting Near-Field Structures Related to Noise Production in High Speed Jets, SciTech paper ref. no. 2323232, 2016.
- [13] Kan, P., Ruscher, C.J., Lewalle, J., and Gogineni, S., Near-field shock/shear-layer interactions in a simulated three-stream supersonic rectangular jet, *Under Review AIAA Journal*, 2017
- [14] Richard, H. and Raffel, M., Principle and applications of the background oriented schlieren (BOS) method, *Measurement Science and Technology*, 2001 vol. 12, No. 9
- [15] Magstadt, A.S., Berry, M.G., Coleman, T.J., Shea, P.R., Glauser, M.N., Ruscher, C.J., Gogineni, S.P. and Kiel, B.V., A near-field investigation of a supersonic, multi-stream jet: locating turbulence mechanisms through velocity and density measurements, SciTech paper, 2016.
- [16] Powell, A., On the Edgetone, *The Journal of the Acoustical Society of America*, Vol. 33, pp 395-409, 1961
- [17] Matthew G. Berry; Andrew S. Magstadt; Mark N. Glauser; Christopher J. Ruscher; Sivaram P. Gogineni; Barry V. Kiel Time-resolved schlieren POD and aft deck pressure correlations on complex supersonic jet nozzles SciTech Paper, 2017
- [18] Dosanjh, D. S., Ahuja, K. K., Bassiouni, M. R. and Bhutiani, P. K., Some recent developments in supersonic jet noise reduction, 2nd *Aeroacoustics Conference*, AIAA-1975-502, 1975.
- [19] Ruscher, C.J., Gogineni, S.P., Viswanath, K., Kiel, B.V., Berry, M.G, Magstadt, A.S. and Glauser, M.N., Analysis of a Supersonic 3-Stream Jet Flow, Part I: Nozzle Design, Experiments, and Simulations *AIAA Journal*, 2015
- [20] Ruscher, C.J., Gogineni, S.P., Viswanath, K., Kiel, B.V., Berry, M.G, Magstadt, A.S. and Glauser, M.N., Aeroacoustic Validation of a Simulation for a Complex Nozzle, 51st *AIAA/ASME/SAE/ASEE Joint Propulsion Conference*, 2015.
- [21] Simmons, R. J., Design and Control of a Variable Geometry Turbofan with an Independently Modulated Third Stream, PhD Dissertation, Ohio State University, 2009.